Supplemental Data

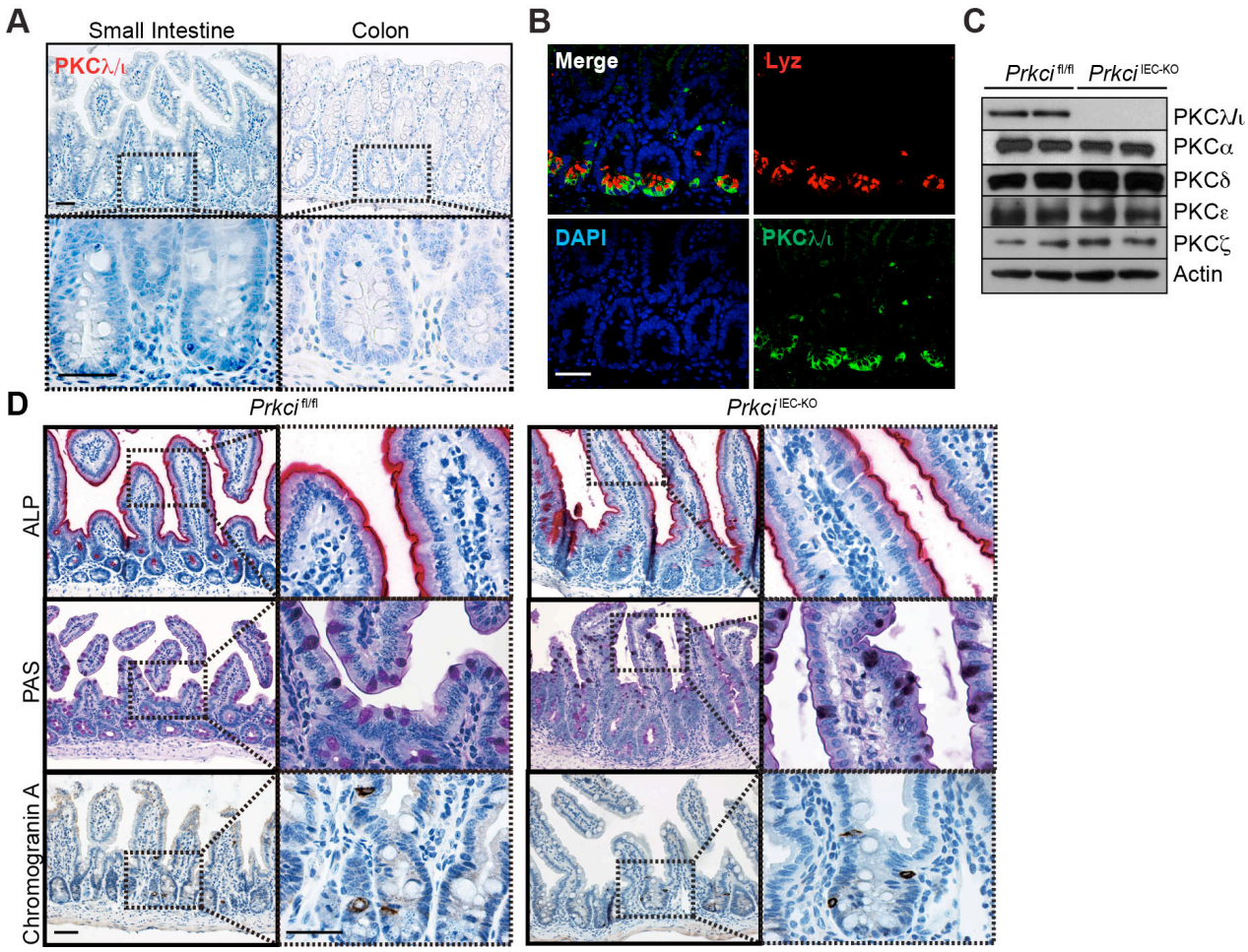

Figure S1, related to Figure 1. Phenotypic characterization of *Prkci*$^{IEC\text{-}KO}$ intestines

(A) IHC for PKCλ/ι of small intestine and colon sections from *Prkci*$^{IEC\text{-}KO}$ mice (n = 3). (B) Double IF for PKCλ/ι (green) and Lysozyme (Lyz; red) of small intestine (n = 3). (C) Immunoblot analysis of PKC isoforms in intestinal epithelial cells from small intestine of *Prkci*$^{fl/fl}$ and *Prkci*$^{IEC\text{-}KO}$ mice. (D) Alkaline Phosphatase (ALP: top), Periodic acid-Schiff (PAS: middle), and Chromogranin A (bottom) staining of small intestine from *Prkci*$^{fl/fl}$ and *Prkci*$^{IEC\text{-}KO}$ mice (n = 3). Scale bars=50 μm.

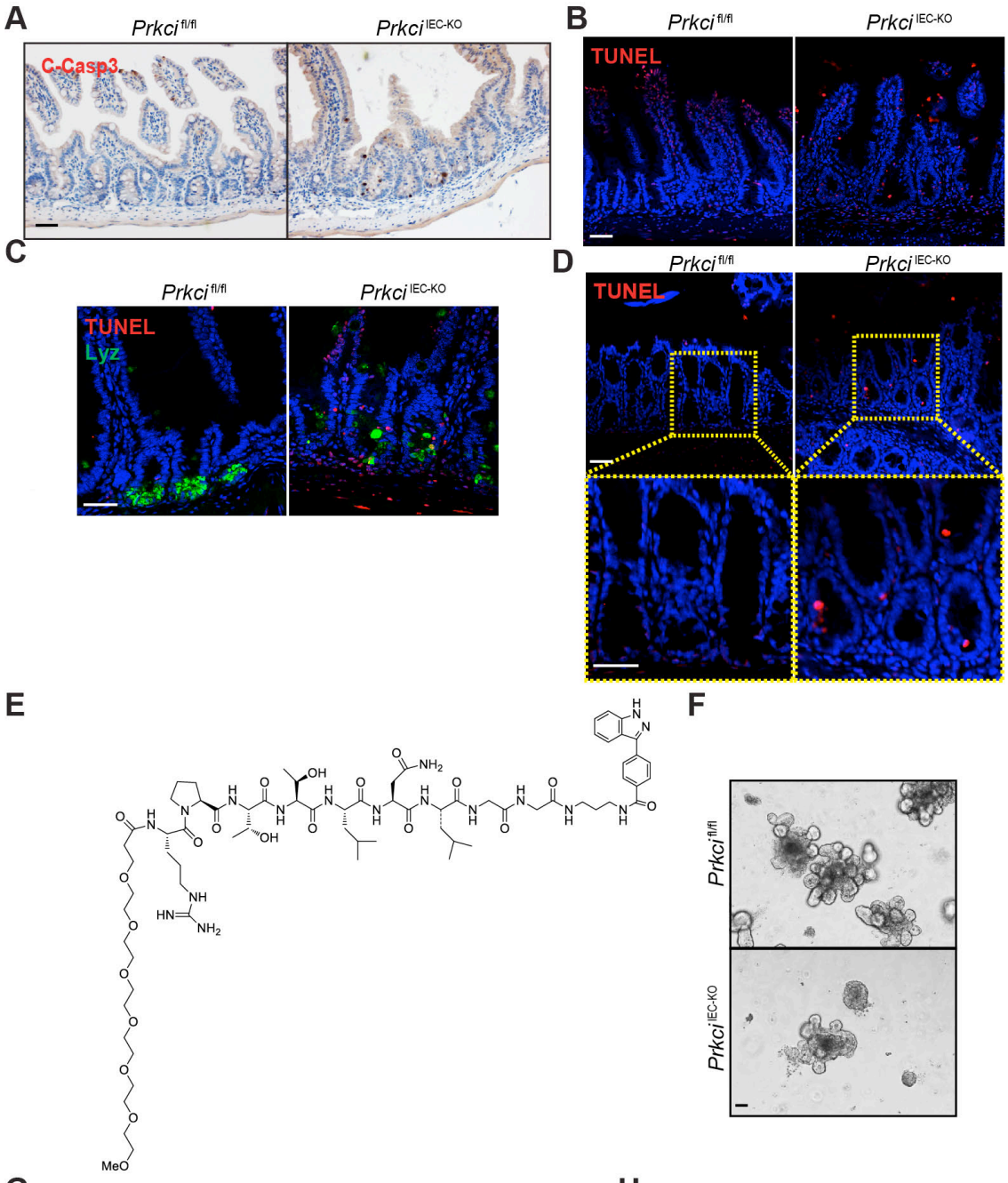
A
Prkci fl/fl
Prkci IEC-KO
C-Casp3
B
Prkci fl/fl
Prkci IEC-KO
TUNEL
C
Prkci fl/fl
Prkci IEC-KO
TUNEL
Lyz
D
Prkci fl/fl
Prkci IEC-KO
TUNEL
E
MeO
F
Prkci fl/fl
Prkci IEC-KO
G
Prkci fl/fl
Prkci IEC-KO
Number of organoids
Number of organoids (> 100 μm)
Average size (μm)
**
**
****
H
Prkci fl/fl
Prkci IEC-KO
Organoid structure (%)
Org 3+
Org 2
Org 1
Sphere

Figure S2, related to Figure 2. Increased epithelial cell death and impaired organoid formation in *Prkci*$^{IEC\text{-}KO}$ mice

(A) IHC for cleaved-caspase 3 (C-Casp3) in *Prkci*$^{fl/fl}$ and *Prkci*$^{IEC\text{-}KO}$ small intestine (n = 3). (B) IF for TUNEL (red) of small intestinal sections (n = 3). (C) Double IF for TUNEL (red) and Lysozyme (Lyz; green) in *Prkci*$^{fl/fl}$ and *Prkci*$^{IEC\text{-}KO}$ small intestine. (D) IF for TUNEL (red) of *Prkci*$^{fl/fl}$ and *Prkci*$^{IEC\text{-}KO}$ colon sections (n = 3). (E) Chemical structure of 126F4. Conjugation of an indozole based ATP mimetic to a minimal JIP1 peptide of sequence RPTTLNL with a di-glycine followed by a 1,4, di-amino butane linker led to a potent and selective dual ATP and substrate JNK inhibitor, with an IC50 value in displacing the JIP peptide of approximately 1 nM. Coupling of the agent with a poly-ethylene glycol moiety further increased the pharmacological properties of the agent. (F) Representative images of small intestine organoids from *Prkci*$^{fl/fl}$ and *Prkci*$^{IEC\text{-}KO}$ mice after 3 days in culture. (G and H) Quantification of number and size (G) and structural complexity of organoids (H). Org 3+: The number of buds ≥ 3, Org 2: The number of buds = 2, Org 1: The number of buds = 1, Sphere: no budding. A minimum of 500 organoids were counted for each group. Scale bars=50 μm. Results are means ± S.E. $^{**}p<0.01$, $^{****}p<0.001$.

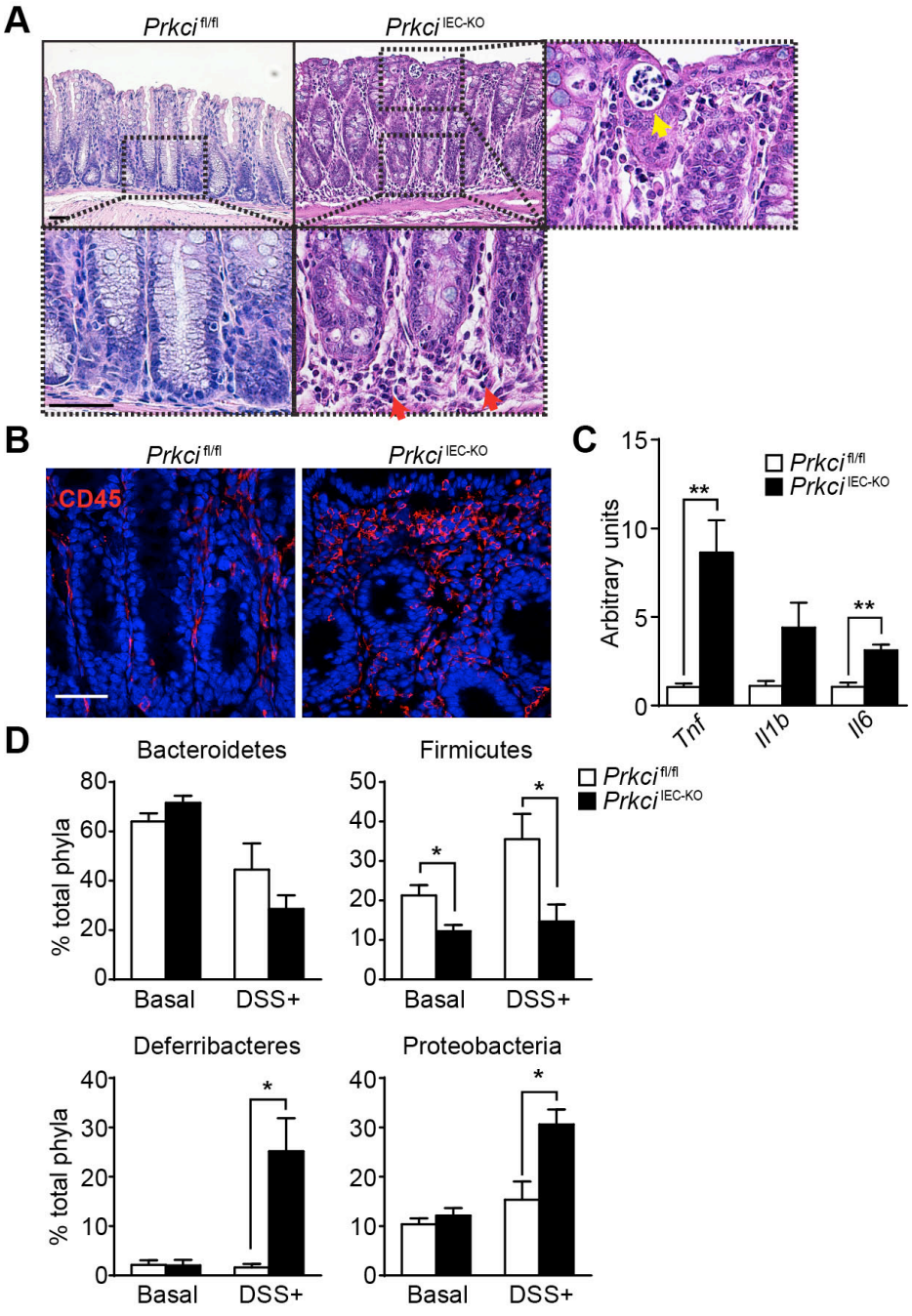

Figure S3, related to Figure 3. Loss of PKCλ/ι leads to colitis and microbial dysbiosis

(A) H&E staining of colon sections from *Prkci*$^{fl/fl}$ and *Prkci*$^{IEC-KO}$ mice (n = 6). Red arrows point to immune cell infiltrates. Yellow arrow points to microabscess. (B) IF for CD45 in *Prkci*$^{fl/fl}$ and *Prkci*$^{IEC-KO}$ colon sections (n = 4). (C) qPCR analysis of mRNA levels of inflammatory cytokines in colon of *Prkci*$^{fl/fl}$ and *Prkci*$^{IEC-KO}$ mice (n = 6). (D) Percentage of each phyla analyzed by 16SrDNA pyrosequencing of fecal pellets in basal conditions and after DSS treatment in *Prkci*$^{fl/fl}$ and *Prkci*$^{IEC-KO}$ mice (n = 8). Scale bars=50 μm. Results are means ± S.E. *p<0.05.

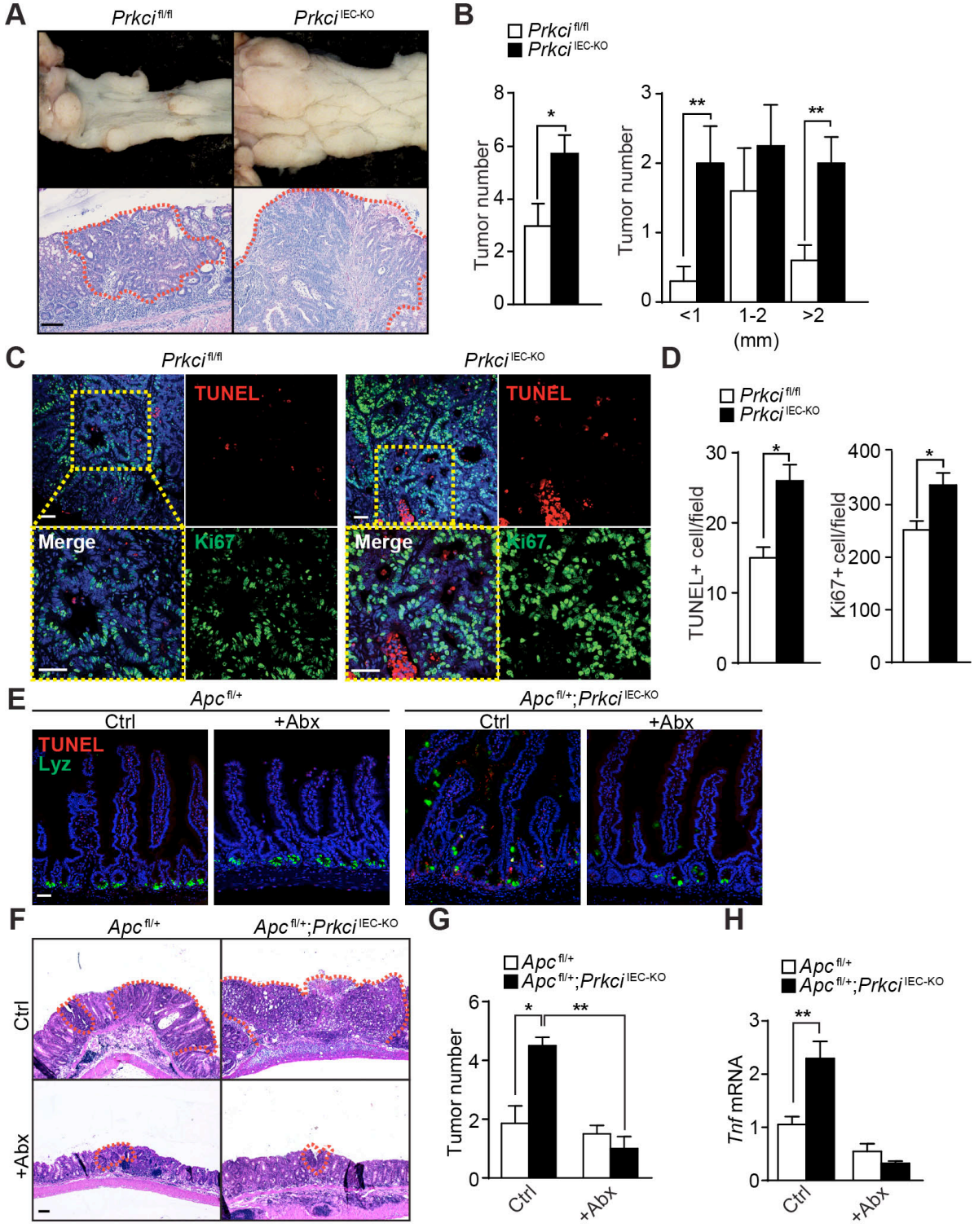
A
Prkci fl/fl
Prkci IEC-KO
B
Prkci fl/fl
Prkci IEC-KO
Tumor number
<1
1-2
>2
(mm)
C
Prkci fl/fl
Prkci IEC-KO
TUNEL
Merge
Ki67
D
TUNEL+ cell/field
Ki67+ cell/field
E
Apc fl/+
Apc fl/+;Prkci IEC-KO
Ctrl
+Abx
TUNEL
Lyz
F
G
Tumor number
H
Tnf mRNA

Figure S4, related to Figure 4. Enhanced tumorigenesis by loss of PKCλ/ι in colitis-associated CRC

(A) Macroscopic image (top) and H&E staining (bottom) of colonic tumors induced by AOM-DSS treatment of *Prkci*$^{fl/fl}$ and *Prkci*$^{IEC\text{-}KO}$ mice (n = 6). Red dashed lines mark the tumor areas. Mice were sacrificed and analyzed 10 weeks after AOM administration. (B) Quantification of the total tumor numbers and stratification of tumors according to size (n = 8). (C) Double IF for TUNEL (red) and Ki67 (green) in AOM/DSS-induced colonic tumors from *Prkci*$^{fl/fl}$ and *Prkci*$^{IEC\text{-}KO}$ mice (n = 3). (D) Quantification of the number of TUNEL- and Ki67-positive cells per field. (E) Double IF for Lysozyme (Lyz; green) and TUNEL (red) in non-tumor lesions of *Apc*$^{fl/+}$ and *Apc*$^{fl/+}$;*Prkci*$^{IEC\text{-}KO}$ small intestine with or without antibiotic (Abx) treatment (n = 3). (F) H&E staining of colon tumors from *Apc*$^{fl/+}$ and *Apc*$^{fl/+}$;*Prkci*$^{IEC\text{-}KO}$ mice with or without Abx treatment (n = 5). Red dashed lines mark the tumor areas. (G) Quantification of the number of colon tumors (n = 5-7). (H) qPCR analysis of *Tnf* mRNA levels in the tumors of *Apc*$^{fl/+}$ and *Apc*$^{fl/+}$;*Prkci*$^{IEC\text{-}KO}$ small intestine (n = 6). Scale bars=50 μm. Results are means ± S.E. *p<0.05, **p<0.01.

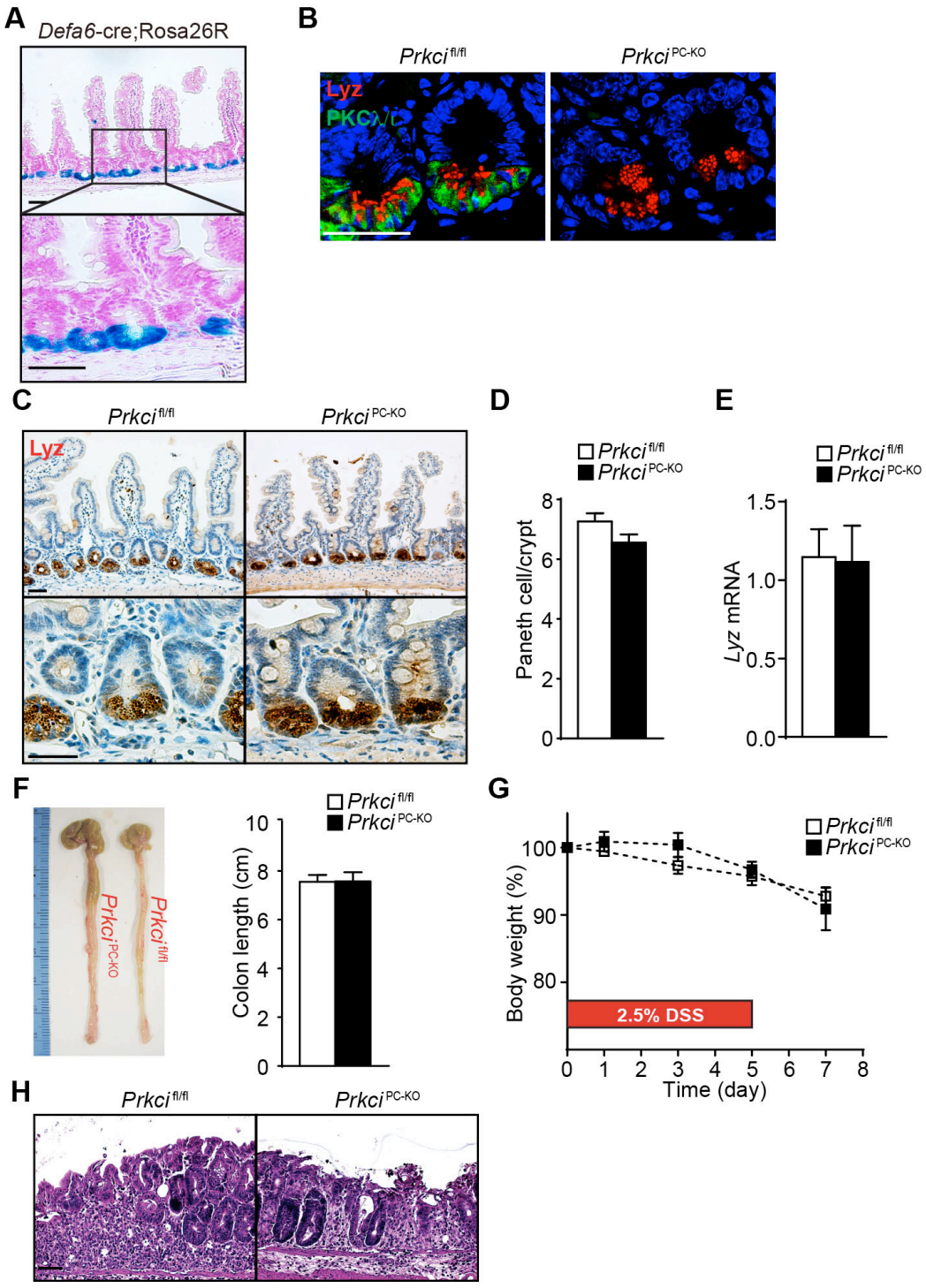

Figure S5, related to Figure 5. Loss of PKCλ/ι in terminally-differentiated Paneth cell does not induce Paneth cell alterations or intestinal inflammation

(A) Xgal staining of small intestine from *Defa6-cre;Rosa26R* mice (n = 3). LacZ-positive cells are blue. Fast Red was used as a nuclear counterstain. (B) Double IF for Lysozyme (Lyz: red) and PKCλ/ι (green) in small intestine crypts from *Prkci*$^{fl/fl}$ and *Prkci*$^{PC\text{-}KO}$ mice (n = 3). (C) IHC for Lyz in small intestine sections from *Prkci*$^{fl/fl}$ and *Prkci*$^{PC\text{-}KO}$ mice (n = 6). (D) Quantification of Lyz-positive Paneth cells per crypt of *Prkci*$^{fl/fl}$ and *Prkci*$^{IEC\text{-}KO}$ mice (n = 6). (E) Quantification of Lyz mRNA levels by qPCR in crypts of *Prkci*$^{fl/fl}$ and *Prkci*$^{PC\text{-}KO}$ mice (n = 6). (F-H) Representative pictures and quantification of colon length (F), change of body weight (G), and H&E staining (H) of colon sections from *Prkci*$^{fl/fl}$ and *Prkci*$^{IEC\text{-}KO}$ mice (n = 5) subjected to a DSS-induced colitis model. Scale bars=50 μm. Results are means ± S.E.

PKCλ/ι phosphorylation sites in EZH2

Amino acid	Phospho (STY) Probabilities in Peptide	Intensity
T487	ESSIIAPAPAEDVDT(1)PPRKK	3.03E+08
S44	SMFS(1)S(1)NRQK	9.12E+07
S40	S(1)MFS(0.017)S(0.983)NRQK	4.17E+07
S690	IRFANHS(1)VNPNCYAK	3.90E+07
T345	EFAAALTAERIKT(1)PPK	3.32E+07

Figure S6, related to Figure 6. EZH2 phosphorylation by PKCλ/ι
PKCλ/ι phosphorylation sites identified in EZH2 by MS/MS analysis.

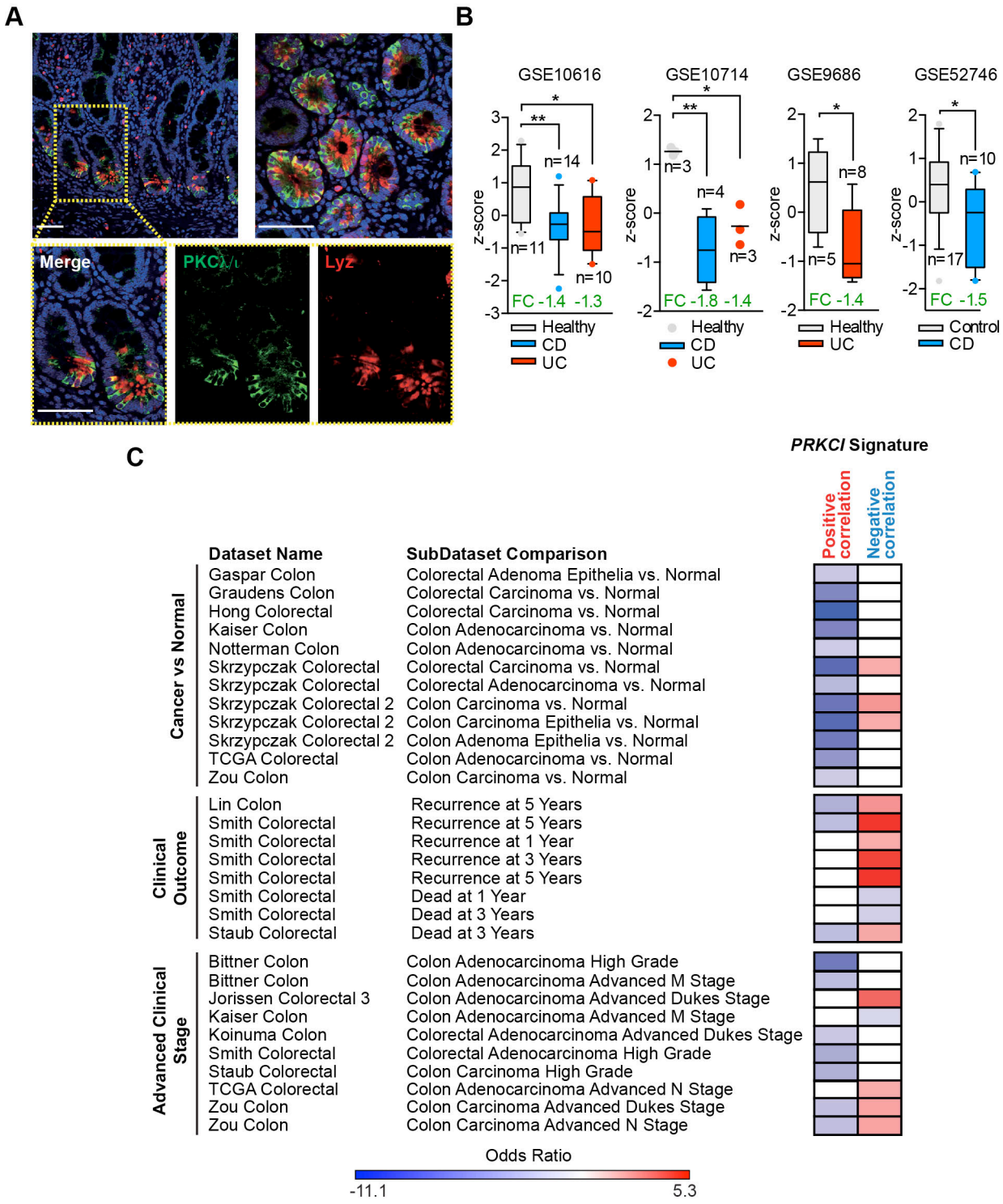

Figure S7, related to Figure 7. Clinical relevance of PKCλ/ι in IBD

(A) Double immunofluorescence for Lysozyme (Lyz: red) and PKCλ/ι (green) in ileum sections from patients with Crohn's disease (n = 10). (B) *PRKCI* mRNA levels in IBD patient samples including Crohn's disease (CD) and ulcerative colitis (UC). Data were collected from public gene expression data sets. (C) Heatmap representation of comparisons between coexpression gene signatures of *PRKCI* from GSE59071 and molecular concepts from the Oncomine database. Associations with overexpression and underexpression concepts reaching odds ratio>2.0 and q-value<0.05 are colored red and blue, respectively. Associations that do not reach the significance threshold are left white. Scale bars=50 µm. Results are means ± S.E. **p*<0.05, ***p*<0.01.

Table S1, Primer sets related to Experimental Procedures.

	Forward	Reverse
18s	GTAACCCGTTGAACCCATT	CCATCCAATCGGTAGTAGCG
Lyz	TGACATCACTGCAGCCATAC	TGGGACAGATCTCGGTTTTG
Egf	TGGCCGGAGAATCTACTGGA	GATGATGCTTCCCGCTCAGA
Defa6	AATCCTCCTCTCTGCCCTCG	GAAGTGCCTTCTGGGTCTCC
Mmp7	AGGCGGAGATGCTCACTTTG	CAAATTCATGGGTGGCAGCA
Muc2	GGTCCAGGGTCTGGATCACA	GCTCAGCTCACTGCCATCTG
Alpi	TCCTACACCTCCATTCTCTATGG	CCGCCTGCTGCTTGTAG
Tnf	CATCTTCTCAAAATTCGAGTGACAA	TGGGAGTAGACAAGGTACAACCC
Il1β	CCCAAGCAATACCCAAAGAA	GGGGAACTCTGCAGACTCAA
Il6	TTCCATCCAGTTGCCTTCTTGG	TTCTCATTTCCACGATTTCCCAG
Il4	ACAGGAGAAGGGACGCCAT	GAAGCCCTACAGACGAGCTCA
Il13	GGAGCTGAGCAACATCACACA	GGTCCTGTAGATGGCATTGCA
Il17f	TTG ATG CAG CCT GAG TGT CT	AAT TCC AGA ACC GCT CCA GT
Il22	GTGAGAAGCTAACGTCCATC	GTCTACCTCTGGTCTCATGG
Ifnγ	ACTGTGATTGCGGGGTTGTA	CCTCCCATCAGCAGCACCT
Atoh1	GTAAGGAGAAGCGGCTGTG	AGCCAAGCTCGTCCACTA
Gfi1	AGAAGGCGCACAGCTATCAC	GGCTCCATTTTCGACTCGC
Atoh1-ChIP-qPCR	GTTGTTGTTCGGGGCTTATC	GGTCCCCCAACTCTTTTACC
Gfi1-ChIP-qPCR	GGGGTTGAGAAGGCTAGTGA	CACCGAGCTCTGAGAGTGTG

Supplemental Experimental Procedures

Antibodies and Reagents

Reagents were obtained from the following sources: recombinant murine EGF, Noggin, and IFNγ were from Peprotech, Inc.; recombinant human TNFα was from Promega; recombinant murine R-Spondin 1 from R&D Systems; Y-27632, cycloheximide (CHX), azoxymethane (AOM), neomycin, metronidazole, vancomycin, Periodic acid-Schiff (PAS) staining kit, and alcian blue solution from Sigma-Aldrich; ampicillin from Fisher Bioreagent; and growth Factor-Reduced Matrigel from BD Bioscience. Advanced DMEM/F12, Glutamax, N2 supplement, and B27 supplement were from Life Technologies; GSK126 from Cayman Chemical Company; dextran sodium sulphate (DSS) from MP Biomedicals; and protein A sepharose 4 fast flow from GE Healthcare Life Sciences. Primary antibodies against PKCλ/ι and CD45 were obtained from BD bioscience; PKCα antibody from Cell Biology; Cleaved-Caspase3, EZH2, PKCζ, and phospho c-Jun from Cell Signaling Technology; β -actin antibody from Sigma-Aldrich; PKCδ, Chromogranin A, F4/80, and H3K27me3 from Abcam; Rabbit anti-Lysozyme antibody from Dako; Gr-1 antibody from R&D Systems; Antibodies against PKCε, HA, and Lysozyme (produced from Goat) from Santa Cruz Biotechnology; and Ki67 and phospho JNK antibodies were from Thermo Scientific. The pCMV-HA-hEZH2 plasmid was obtained from Addgene, plasmid #24230 (Pasini et al., 2004). Recombinant PKCλ/ι was obtained from Upstate.

Mice

Prkci$^{fl/fl}$ (Leitges et al., 2001), *Apc*$^{fl/fl}$ (Hinoi et al., 2007), *Villin*-cre (el Marjou et al., 2004; Madison et al., 2002), *Defa6*-cre (Adolph et al., 2013), and Rosa26R (Barker et al., 2007) mice were previously described. Mice were sacrificed and small intestines and colons were collected for analyses. Mice were maintained under controlled temperature (22.5 °C) and illumination (12 hr dark/light cycle), and were age-matched as well as co-housed for all experiments. All genotyping was done by PCR. Littermate male mice were analyzed in all the experiments. Mice were sacrificed at age of eight weeks, unless otherwise indicated. *Prkci*$^{IEC\text{-}KO}$ mice were generated by crossing *Villin*-cre heterozygotes mice with *Prkci*$^{fl/fl}$ mice, and maintained by crossing *Prkci*$^{IEC\text{-}KO}$ mice with *Prkci*$^{fl/fl}$ mice. *Apc*$^{fl/+}$;*Prkci*$^{IEC\text{-}KO}$ mice were generated by crossing *Prkci*$^{IEC\text{-}KO}$ mice with *Apc*$^{fl/fl}$ mice, and maintained by crossing *Apc*$^{fl/+}$;*Prkci*$^{IEC\text{-}KO}$ mice with either *Prkci*$^{fl/fl}$ mice, *Apc*$^{fl/+}$;*Prkci*$^{fl/fl}$ mice, or *Apc*$^{fl/fl}$;*Prkci*$^{fl/fl}$ mice. *Apc*$^{fl/+}$ control mice were generated and maintained by crossing *Villin*-cre heterozygotes mice with *Apc*$^{fl/fl}$ mice. Experimental colitis was induced by treating 8-week-old mice with 2.5% DSS in the drinking water for 5 days, followed by a 48 hr recovery period with regular drinking water through the end of the experiment. DSS-containing water was exchanged every other day. Mice were examined by measuring body weight loss and water consumption and by monitoring development of diarrhea and rectal bleeding. To examine the tumorigenesis in Apc flox tumor model, 20-week-old *Apc*$^{fl/+}$ control or *Apc*$^{fl/+}$;*Prkci*$^{IEC\text{-}KO}$ mice were sacrificed and analyzed. For antibiotic treatment, 12-week-old *Apc*$^{fl/+}$ control or *Apc*$^{fl/+}$;*Prkci*$^{IEC\text{-}KO}$ mice were administrated a combination of ampicillin (1 g/L), neomycin (1 g/L), metronidazole (1 g/L), and vancomycin (0.5 g/L) in drinking water for 8 weeks until they were sacrificed at the age of 20 weeks. For the AOM/DSS tumor-developing experiment, 10- to 12-week-old mice were injected intraperitoneally with a single dose of AOM (10 mg/kg) in sterile PBS. After 5 days, 2% DSS was given in the drinking water for 5 days, followed by 14 days of regular drinking water. The DSS treatment was repeated for two additional cycles, and mice were sacrificed 70 days after the AOM injection. The Institutional Animal Care and Utilization Committee approved all procedures, in accordance with the NIH guide for the care and use of laboratory animals.

Histology, Immunohistochemistry, Immunofluorescence, and Electron microscopy.

Intestines were isolated, rinsed in ice-cold PBS, fixed in 10% neutral buffered formalin overnight at 4°C, dehydrated, and embedded in paraffin. Sections (5 μm) were stained with hematoxylin and eosin (H&E). For immunohistochemistry, sections were deparaffinized, rehydrated, and then treated for antigen retrieval. After blocking in avidin/biotin solutions (Vector Laboratories), tissues were incubated with primary antibody overnight at 4°C followed by incubation with biotinylated secondary antibody. Endogenous peroxidase was quenched in 3% H_2O_2 in water for 10 min at room temperature. Antibodies were visualized with avidin/biotin complex (Vectastain Elite; Vector Laboratories) using diaminobenzidine as the chromagen. For immunofluorescence, sections were incubated with Alexa-conjugated secondary antibodies (Life Technologies) and the samples examined with a Zeiss LSM 710 NLO Confocal Microscope. Cell death was analyzed using the in situ cell death detection kit, TMR red (Roche) for TUNEL. Periodic acid-Schiff reagent (PAS) and alcian blue staining were performed according to standard protocols. Staining for Periodic acid-Schiff reagent (PAS), Alkaline phosphatase (ALP), and β-

galactosidase (LacZ) were previously described (Llado et al., 2015). For electron microscopy, glutaraldehyde-fixed material was used. After embedding in Epon Araldite, ultrathin sections were cut and examined using a Philips CM-100 Transmission Electron Microscope.

Crypt and Intestinal Epithelial Cell Isolation and Small Intestine Organoid Culture

Crypt isolation and intestinal epithelial cell (IEC) isolation were performed as described previously (Llado et al., 2015). Isolated crypts or IECs were pelleted and then lysed for RNA extraction or immunoblotting. For small intestine organoid culture, crypt number was counted after isolation and a total of 300 crypts were mixed with 50 μl of Matrigel and plated in 48-well plates. After polymerization of Matrigel, 300 μl of crypt culture medium (Advanced DMEM/F12 containing 10 mM HEPES, 1X Glutamax, 1X N2 supplement, 1X B27 supplement, 50 ng/ml EGF, 1000 ng/ml R-spondin1, 100 ng/ml Noggin, and 10 μM Y-2763) was added. In some experiments, organoids were treated with recombinant human TNFα (10 ng/ml), murine IFNγ (100 ng/ml), 126F4 (50 μM), or GSK126 (2 μM) for the indicated duration.

Bacterial DNA extraction and 16S sequencing

Mouse stool samples were collected fresh and pellets were frozen on dry ice and stored at -80°C until use. The bacterial DNA was extracted using the QIAmp Fast DNA Stool Mini Kit (QiAGEN), with the addition of a bead-beating step. In order to ensure uniform lysis of bacterial cells, fecal pellets were beaten with glass beads for 5 min in InhibitEX buffer (included in QIAamp Fast Stool Mini Kit) using Mini-Beadbeater-16 (Biospec Products). Library preparation was performed following instructions written by Illumina, found in the 16S Metagenomic Sequencing Library Preparation. As described in this guide, the V3-V4 region of the bacterial 16S ribosomal DNA was amplified with PCR using Forward: 5'-TCGTCG GCAGCGTCAGATGTGTATAAGAGACAGCCTACGGGNGGCWGCAG and Reverse: 5'-GTCTCGTGGGCTCGGAGATGTGTATAAGAGACAGGACTACHVGGGTATCTAATCC. Adapter and barcode sequences for dual indexing were also used as described in the 16S Metagenomic Sequencing Library Preparation protocol. PCR clean-up steps were done with QIAquick 96-PCR Clean-up kit (QIAgen), and library quantification was done using KAPA Library Quantification Kit for Illumina platforms (KAPA Biosystems). The Experion system (Bio-rad) was used to analyze the DNA concentration and purity of pooled libraries. Prepared 16S libraries were sent to the Genomics Core, SBP, Lake Nona, FL for analysis on the MiSeq platform (Illumina). Demultiplexing, trimming of primers, adapters, and barcode sequences were done by the Genomics Core, SBP, Lake Nona, FL using Illumina software. Sequences were subsequently analyzed in the lab using the pipeline Qiime 1.9.1 (Caporaso et al., 2010b); operational taxonomic Units (OTUs) were picked based on 97% sequence similarity with uclust (Edgar, 2010), and PyNAST (Caporaso et al., 2010a) was used to align representative OTUs to GreenGenes 13_8 (McDonald et al., 2012) and the RDP classifier 2.2 (Wang et al., 2007) was used to assign taxonomy.

JNK inhibitor

The JNK inhibitor 126F4 was, like the previously reported DJNKI-1 (Barr et al., 2002; Bonny et al., 2001), generated to attenuate JNK activation by binding the JIP binding site that is essential for both substrate recognition and activation of JNK by upstream kinases (Barr et al., 2002; Bonny et al., 2001; Stebbins et al., 2008). However, DJNKI-1 presents two limitations, namely poor affinity for JNK and poor cell permeability, given its peptide nature. Hence, we recently reported on bi-dentate molecules that were designed to span both the JIP binding site and the ATP binding site (Stebbins et al., 2011). The resulting bi-dentate agents were orders of magnitude more potent than DJNKI-1 and competitive against both the cofactor ATP and JNK substrates in the single digit nanomolar range (Stebbins et al., 2011). To further enhance the cell-permeability of these bi-dentate JNK inhibitors, we conjugated our previously reported agent, namely compound 9 (Stebbins et al., 2011) with a short poly(ethylene glycol) (PEG) chain, instead of the HIV-TAT sequence used in DJNKI-1. PEGylated molecules present overall improved pharmacological properties and numerous PEG-based therapeutics have been developed (Banerjee et al., 2012). The synthesis and purification of 126F4 was accomplished using a similar strategy as reported in Stebbins et al. 2011, starting from commercially available indazole and natural aminoacyls, to obtain bi-dentate compound 9 (Stebbins et al., 2011). Final compound was obtained by coupling of a poly-ethylene glycol acid tag of sequence CH3O(CH2CH2O)7CH2CH2COOH to N-terminus of compound 9, to yield to 126F4. The final product was obtained by HPLC purification using an Atlantis Preparative T3 column (10 x 250 mm), acetonitrile-water system, RT~ 12 min, purity > 95%.

Cell Culture Procedures

HEK293T and SW480 cells were purchased from ATCC and were cultured in DMEM supplemented with 10% FCS,

2 mM L-glutamine, 100 U/ml penicillin, and 100 μg/ml streptomycin. To knock down PKCλ/ι in SW480 cells, TRC lentiviral shRNA targeting human PKCλ/ι (TRCN0000022757) was obtained from Open Biosystems. shRNA-encoding plasmids were co-transfected with psPAX2 (Addgene; plasmid 12260; Trono Lab Packaging and Envelope Plasmids, unpublished) and pMD2.G (Addgene; plasmid 12259 Trono Lab Packaging and Envelope Plasmids, unpublished) packaging plasmids into actively growing HEK293T cells by using XtremeGene HP transfection reagent (Roche). Virus-containing supernatants were collected 48 hr after transfection, filtered to eliminate cells, and then used to infect SW480 cells in the presence of 8 μg/ml polybrene (Millipore). Cells were analyzed on the third day after infection to confirm knockdown. For TNFα stimulation, recombinant human TNFα (10 ng/ml) was added to the culture medium and protein was collected at the indicated time points. For cell death rescue experiments, cells were pretreated with DMSO or JNK inhibitor (50 μM) for 30 min, followed by addition of TNFα (10 ng/ml) and CHX (25 μg/ml). After 4 hr incubation, protein was extracted and analyzed by immunoblotting.

To knock out PKCλ/ι in HEK293T cells, a 20-nucleotide single-guide RNA sequence targeting the first exon of the human PRKCI gene (5' GCCGCCGCCTGCGACCGTGT) was designed using the CRISPR design tool at http://crispr.mit.edu/ and cloned into a bicistronic expression vector containing human codon-optimized Cas9 fused to EGFP through the T2A sequence and the tracrRNA components (Addgene #48138), (Ran et al., 2013), creating the construct sgPRKCI-PX458. sgPRKCI-PX458 was transfected into HEK293T cells using Lipofectamine 2000 according to the manufacturer's instructions. 24 hr post transfection, the cells were trypsinized, washed with PBS, and re-suspended in FACS sorting buffer (1% FBS, 1mMEDTA, 25 mM HEPE pH 7.0, in 1X Phosphate Buffered Saline) with addition of propidium iodide. Viable GFP-positive cells were single-sorted by FACS (SBP FACS core, FACS ARIA) into 96-well plates containing DMEM with 20% FBS and 50 μg/ml penicillin/streptomycin. Single clones were expanded and screened for PKCλ/ι expression by protein immunoblotting. For the protein stability assay, CHX (100 μg/ml) was added 24 hr after seeding, and protein was extracted at the indicated time points.

Cell Lysis and Immunoblotting

Cells, organoids, or intestinal extracts were lysed in ice-cold lysis buffer (40 mM HEPES [pH 7.4], 120 mM NaCl, 1 mM EDTA, 10 mM pyrophosphate, 10 mM glycerophosphate, 0.3% CHAPS, and 1 tablet of Roche EDTA free-protease inhibitors per each 25 ml). The soluble fractions of cell lysates were isolated by centrifugation at 13,000 rpm for 15 min. Protein extracts or immunoprecipitated proteins were denatured by the addition of sample buffer and boiling for 5 min, resolved by 8%–14%, SDS-PAGE and then transferred to nitrocellulose-ECL membranes (GE Healthcare).

In Vitro Kinase Assay

Fifteen μg of HA-tagged human EZH2 (HA-EZH2) plasmid was transfected to ~80% confluent HEK293T cells in a P100 format. Cells were lysed in RIPA buffer 48 hr after transfection and HA-EZH2 was immunoprecipitated using anti-HA beads (Sigma). Immunoprecipitates were washed and incubated at 30ºC for 60 min in kinase-assay buffer containing 25 mM Tris-HCl (pH 7.5), 5 mM MgCl2, 0.5 mM EGTA, 1 mM DTT, and 400 μM ATPγS (Biolog) in the presence of recombinant PKCλ/ι. Detection of substrate phosphorylation was performed using the ATP analog-based phosphorylation detection used previously (Allen et al., 2007) with minor modifications. Briefly, after the phosphorylation reaction, PNBM (Abcam) and EDTA were added to a final concentration of 2.5 mM and 20 mM, respectively, and incubated for 1 hr at room temperature. Immunoblotting detection was performed with anti-thiophosphate ester antibody (Abcam).

Chromatin Immunoprecipitation (ChIP) Analysis

Isolated crypt cells from *Prkci*$^{fl/fl}$ and *Prkci*$^{IEC\text{-}KO}$ mice were fixed in 1% formaldehyde in PBS for 10 min at RT, and 25 M Glycine was added to final concentration of 125 mM glycine. After 5 min incubation, fixed cells were washed with ice-cold PBS and lysed with cell lysis buffer (1 M Tris pH 8.0, 10 mM NaCl, 0.5% NP-40, and protease inhibitors). After 15 min incubation, crypt cell lysate was centrifuged and supernatant was removed. Pellets were lysed with nuclear lysis buffer (50 mM Tris pH 8.0, 10 mM EDTA, 1% SDS and protease inhibitors) and incubated for 30 min at 4ºC. Chromatin was sheared in a COVARIS S220 Focused-ultra sonicator to yield DNA fragment sizes of 200–1000 base pairs, and diluted 10 times in dilution buffer (20 mM Tris pH 8.0, 2 mM EDTA, 1% triton X-100, 150 mM NaCl and protease inhibitors). The DNA was quantified by using Nanodrop 1000 spectrophotometer and 60–100 ng of DNA was used for each ChIP experiment. Immunoprecipitations were carried out overnight at 4°C using the antibodies for EZH2 or H3K27me3, and pulled-down by 20 μl of a 50% slurry of protein A-sepharose. Immunocomplexes were washed sequentially with buffer TSEI (20 mM Tris pH 8.0, 2 mM

EDTA, 1% triton X-100, 150 mM NaCl, 0.1% SDS, and protease inhibitors), buffer TSEII (20 mM Tris pH 8.0, 2 mM EDTA, 1% triton X-100, 500 mM NaCl, 0.1% SDS, and protease inhibitors), buffer TSEIII (10 mM Tris pH 8.0, 250 mM LiCl, 1 mM EDTA, 1% NP40, 1% Deoxycholate, and protease inhibitors) and TE buffer (10 mM Tris pH 8.0, 1 mM EDTA). Immunocomplexes were eluted in TE containing 1% SDS, and protein–DNA cross-links were reverted by heating at 65°C overnight. After RNase treatment and proteinase K digestion, DNA was extracted by using a PCR purification kit (Qiagen). One-tenth of the immunoprecipitated DNA was used in each PCR, for which the promoter-specific primers described in Table S1 were used.

RNA Extraction and Analyses

Total RNA from mouse tissues and cultured organoids was extracted using the RNeasy Mini Kit (QIAGEN), following the manufacturer's instruction. After quantification using a Nanodrop 1000 spectrophotometer (Thermo Scientific), 1 µg of RNA was reverse-transcribed using random primers and MultiScribe Reverse Transcriptase (Applied Biosystems). Gene expression was analyzed by amplifying 50 ng of the complementary DNA using the CFX96 Real-Time PCR Detection System with SYBR Green Master Mix (BioRad) and primers described in Table S1. The amplification parameters were set at 95ºC for 30 s, 58ºC for 30 s, and 72ºC for 30 s (40 cycles in total). Gene expression values for each sample were normalized to the 18S RNA.

Array and Gene Set Enrichment Analysis

Microarray studies were performed in the Genomics Core at SBP Medical Discovery Institute. Briefly, total RNA was extracted from isolated crypt cells from 3 independent *Prkci*$^{fl/fl}$ and *Prkci*$^{IEC\text{-}KO}$ mice and hybridized on Affymetrix mouse ST 1.0 microarrays. Scanning of the images and the first-pass processing of probe-level fluorescence intensities were performed using the Microarray Suite 5.0 software (MAS 5.0; Affymterix, Santa Clara, CA). The data were normalized, and calculation of the gene-specific summary measures was performed by the robust multi-array average (RMA) procedure (Irizarry et al., 2003) based on the Entrez gene-centric probe set definitions provided by the University of Michigan "brainarray" group (Dai et al., 2005). The statistical significance of differential gene expression between *Prkci*$^{fl/fl}$ and *Prkci*$^{IEC\text{-}KO}$ crypts was assessed using Comparative Marker Selection (GenePattern, Broad Institute). Gene set enrichment analysis was performed using GSEA v2.0.14 software (http://www.broadinstitute.org/gsea/index.jsp) with 5000 gene-set permutations using the gene-ranking metric T-test with Hallmark MSigDb collection (Subramanian et al., 2005). Heat-map representation of gene expression was generated using GENE-E (Broad Institute). Meta-analyses to identify overlapping and associated genes with publically available data set were performed using the NextBioTM (Illumina) on-line search engine (www.nextbio.com).

Bioinformatic Analysis of Clinical Data

Meta-analysis of *PRKCI* gene expression in Crohn's disease and ulcerative colitis datasets was performed using NextBio. Raw gene expression data from relevant datasets were directly accessed through the GEO website (NCBI). Levels of *PRKCI* gene expression were converted to z-scores and differential expression was assessed by t-test comparisons. *PRKCI* gene signatures were generated by computing Pearson correlation coefficients of *PRKCI* with every gene in GSE59071. TOP-400 most correlated and anti-correlated genes with *PRKCI* were used as "Concept" genesets and uploaded to Oncomine (www.oncomine.com) for further analysis. Survival plots of *PRKCI*-stratified colorectal cancer patients (Smith Colorectal) were obtained using PRECOG (Gentles et al., 2015).

Supplemental References

Allen, J.J., Li, M., Brinkworth, C.S., Paulson, J.L., Wang, D., Hubner, A., Chou, W.H., Davis, R.J., Burlingame, A.L., Messing, R.O., et al. (2007). A semisynthetic epitope for kinase substrates. Nat Methods 4, 511-516.

Banerjee, S.S., Aher, N., Patil, R., and Khandare, J. (2012). Poly(ethylene glycol)-Prodrug Conjugates: Concept, Design, and Applications. J Drug Deliv 2012, 103973.

Barker, N., van Es, J.H., Kuipers, J., Kujala, P., van den Born, M., Cozijnsen, M., Haegebarth, A., Korving, J., Begthel, H., Peters, P.J., et al. (2007). Identification of stem cells in small intestine and colon by marker gene Lgr5. Nature 449, 1003-1007.

Caporaso, J.G., Bittinger, K., Bushman, F.D., DeSantis, T.Z., Andersen, G.L., and Knight, R. (2010a). PyNAST: a flexible tool for aligning sequences to a template alignment. Bioinformatics 26, 266-267.

Caporaso, J.G., Kuczynski, J., Stombaugh, J., Bittinger, K., Bushman, F.D., Costello, E.K., Fierer, N., Pena, A.G., Goodrich, J.K., Gordon, J.I., et al. (2010b). QIIME allows analysis of high-throughput community sequencing data. Nat Methods 7, 335-336.

Dai, M., Wang, P., Boyd, A.D., Kostov, G., Athey, B., Jones, E.G., Bunney, W.E., Myers, R.M., Speed, T.P., Akil, H., et al. (2005). Evolving gene/transcript definitions significantly alter the interpretation of GeneChip data. Nucleic acids research 33, e175.

Edgar, R.C. (2010). Search and clustering orders of magnitude faster than BLAST. Bioinformatics 26, 2460-2461.

el Marjou, F., Janssen, K.P., Chang, B.H., Li, M., Hindie, V., Chan, L., Louvard, D., Chambon, P., Metzger, D., and Robine, S. (2004). Tissue-specific and inducible Cre-mediated recombination in the gut epithelium. Genesis 39, 186-193.

Gentles, A.J., Bratman, S.V., Lee, L.J., Harris, J.P., Feng, W., Nair, R.V., Shultz, D.B., Nair, V.S., Hoang, C.D., West, R.B., et al. (2015). Integrating Tumor and Stromal Gene Expression Signatures With Clinical Indices for Survival Stratification of Early-Stage Non-Small Cell Lung Cancer. J Natl Cancer Inst 107.

Hinoi, T., Akyol, A., Theisen, B.K., Ferguson, D.O., Greenson, J.K., Williams, B.O., Cho, K.R., and Fearon, E.R. (2007). Mouse model of colonic adenoma-carcinoma progression based on somatic Apc inactivation. Cancer Res 67, 9721-9730.

Irizarry, R.A., Hobbs, B., Collin, F., Beazer-Barclay, Y.D., Antonellis, K.J., Scherf, U., and Speed, T.P. (2003). Exploration, normalization, and summaries of high density oligonucleotide array probe level data. Biostatistics 4, 249-264.

Leitges, M., Sanz, L., Martin, P., Duran, A., Braun, U., Garcia, J.F., Camacho, F., Diaz-Meco, M.T., Rennert, P.D., and Moscat, J. (2001). Targeted disruption of the zetaPKC gene results in the impairment of the NF-kappaB pathway. Mol Cell 8, 771-780.

Madison, B.B., Dunbar, L., Qiao, X.T., Braunstein, K., Braunstein, E., and Gumucio, D.L. (2002). Cis elements of the villin gene control expression in restricted domains of the vertical (crypt) and horizontal (duodenum, cecum) axes of the intestine. J Biol Chem 277, 33275-33283.

McDonald, D., Price, M.N., Goodrich, J., Nawrocki, E.P., DeSantis, T.Z., Probst, A., Andersen, G.L., Knight, R., and Hugenholtz, P. (2012). An improved Greengenes taxonomy with explicit ranks for ecological and evolutionary analyses of bacteria and archaea. ISME J 6, 610-618.

Pasini, D., Bracken, A.P., Jensen, M.R., Lazzerini Denchi, E., and Helin, K. (2004). Suz12 is essential for mouse development and for EZH2 histone methyltransferase activity. Embo J 23, 4061-4071.

Ran, F.A., Hsu, P.D., Wright, J., Agarwala, V., Scott, D.A., and Zhang, F. (2013). Genome engineering using the CRISPR-Cas9 system. Nat Protoc 8, 2281-2308.

Stebbins, J.L., De, S.K., Pavlickova, P., Chen, V., Machleidt, T., Chen, L.H., Kuntzen, C., Kitada, S., Karin, M., and Pellecchia, M. (2011). Design and characterization of a potent and selective dual ATP- and substrate-competitive subnanomolar bidentate c-Jun N-terminal kinase (JNK) inhibitor. Journal of medicinal chemistry 54, 6206-6214.

Subramanian, A., Tamayo, P., Mootha, V.K., Mukherjee, S., Ebert, B.L., Gillette, M.A., Paulovich, A., Pomeroy,

S.L., Golub, T.R., Lander, E.S., et al. (2005). Gene set enrichment analysis: a knowledge-based approach for interpreting genome-wide expression profiles. Proc Natl Acad Sci U S A 102, 15545-15550.

Wang, Q., Garrity, G.M., Tiedje, J.M., and Cole, J.R. (2007). Naive Bayesian classifier for rapid assignment of rRNA sequences into the new bacterial taxonomy. Applied and environmental microbiology 73, 5261-5267.